2019-08-15

Aeration effects on water-structure impacts: Part 2. Wave impacts on a truncated vertical wall

Mai, T

10.1016/j.oceaneng.2019.05.035
Ocean Engineering
Elsevier

AERATION EFFECTS ON WATER-STRUCTURE IMPACTS: PART 2. WAVE IMPACTS ON A TRUNCATED VERTICAL WALL

T. Mai [a, b, 1], C. Mai [c], A. Raby [a] and D. M. Greaves [a]

[a] *School of Engineering, University of Plymouth, Plymouth, Devon, PL4 8AA, United Kingdom*
[b] *Now at National University of Civil Engineering, 55 Giai Phong, Hai Ba Trung, Hanoi, Vietnam*
[c] *Thuy Loi University, 175 Tay Son, Dong Da, Hanoi, Vietnam*

ABSTRACT

Aeration effects on wave loading are of considerable importance for offshore design. This paper describes experimental work to investigate four types of wave impact on a truncated vertical wall (representative of a plate in an FPSO vessel), in pure and aerated water. Investigations showed that high aeration and flip-through wave impacts are the most severe impact types and should therefore be considered for offshore structure design. It was also observed that there is a significant reduction in peak impact loads (both pressure and force) for impacts in aerated water compared to those in pure water. However, there was almost no reduction in impulsive loadings in aerated water compared to those in pure water, and therefore maximum instantaneous loads may be conservative in the presence of aerated water, in the implementation for offshore structure design. This paper is a companion paper to "Aeration effects on water-structure impacts: Part 1. Drop plate impacts".

Keywords: aeration effect, wave impact, physical model

1 Introduction

Breaking wave impacts on vertical structures can produce very high loads, which may lead to structural failure and damage. Wave impacts on coastal and offshore structures have been investigated experimentally and numerically for several decades. Most investigations have been carried out to improve understanding of the physics and characteristics of wave impacts on a vertical wall (Chan, 1994; Oumeraci et al., 1992 & 1993; Hattori et al., 1994; Bullock et al., 2007; Bredmose et al., 2010; Hofland et al., 2011; Lafeber et al., 2012; Guilcher et al., 2013; Chuang et al., 2017&2018) or a vertical cylinder (Wienke and Oumeraci, 2005). The physics and characteristics of the impact loading have been shown by researchers to depend significantly on the breaking wave conditions (Oumeraci et al., 1993; Hattori et al., 1994). Hattori et al. (1994) found in their experimental results that the smaller the amount of entrapped air between the breaking wave and the wall at the collision, the higher the impact pressure. However, the distinctions between low-aeration (small amount of entrapped air) and high-aeration (large amount of entrapped air) were considered by Bullock et al. (2007), who found that a high aeration level, which is known as a large air-pocket wave impact, does not always reduce the peak pressure, and indeed can increase both the force and impulse on the structure. The highest impact pressures were found to occur around still water level (SWL) under regular wave conditions by Hattori et al., (1994) and Bullock et al., (2007). Other researchers found the maximum peak pressure occurred at SWL for certain impact types (Chan and Meville, 1988; Chan, 1994; Hull and Müller, 2002; Oumeraci et al., 1993), whereas Hofland et al. (2011) found that the location of the pressure peak was above SWL in their tests. Limited research has been conducted on the effect of aerated water on wave impacts. Kimmoun et al. (2012) carried out experiments to investigate the influence of a bubble curtain on wave impacts on a vertical wall with the soliton and wave focusing techniques. They found that for cases using the wave-focusing technique, the location of the bubble generator and the injected air flow rate affect the wave breaking process; the variation of loads is increased while the area corresponding to the high loads is reduced. In addition, Kimmoun

[1] Corresponding author.

E-mail address: tri.mai@plymouth.ac.uk, trimc@nuce.edu.vn (Tri Mai)

et al. (2012) found that the compressibility of the aerated water does not seem to be of significant influence on wave impacts generated using the soliton wave technique.

Here, we investigate the effects of aeration on wave impact by generating wave impacts of different types on a truncated vertical wall (representing a section of FPSO, Floating Production Storage and Offloading vessel, hull) in pure and aerated water. The companion paper, "Aeration effects on water-structure impacts: Part 1. Drop plate impacts" deals with the related, and perhaps converse problem of a plate hitting an otherwise still water surface.

2 Methodology

2.1 Wave impact test

2.1.1 Physical model of wave impact test

The wave impact experiments were carried out in the Sediment Wave Flume at the University of Plymouth COAST Lab. The flume is 35 m long with a working section 0.6 m wide, 1.2 m high and maximum still water depth of 0.8 m. A schematic of the physical model setup is given in Figure 1. The truncated vertical wall (Plate 1) is an aluminium plate of 0.56 m width by 0.6 m height and 0.012 m thickness connected to rigid plates (Plates 2 and 3). Plates 2 and 3 were mounted on a support frame by a low-profile load cell and Plate 4. There were 0.02 m gaps on both sides of the tested model to ensure no friction between the model and the flume side walls, where such a force would affect load measurement. Pressures under wave impact were measured by FGP XPM10 pressure sensors installed at 7 locations on the impact wall, and a low-profile load cell (stainless steel series) with an inline DC amplifier (Model 140) used to measure the total force on the wall. An accelerometer (Model 4610) was used to measure vibration of the structure under wave impact. Figure 1c presents the configuration of the instrumentation on the impact plate. Pressure, force and acceleration data were sampled at 35 kHz frequency.

Thirteen resistance-type wave gauges were used to measure water elevation along the wave flume, sampled at 128 Hz. In addition, a Photron SA4 high speed camera (frame rate up to 3600 fps at a resolution of 1024x1024) was used to visualise the air pockets, wave run-up and jets produced at impact.

The same bubble generation system was used as for the drop tests to generate aerated water with 0.6% void fraction for these flume tests, located 0 m from the impact wall (Figure 1a, b). The 0.6% aeration level is the lowest aeration level we could produce in our wave flume to minimize distortion of water surface and water flow under tested waves. The bubble generator was switched off for the first condition. Mai (2017) and Mai et al. (2019) present further details of the bubble generation system.

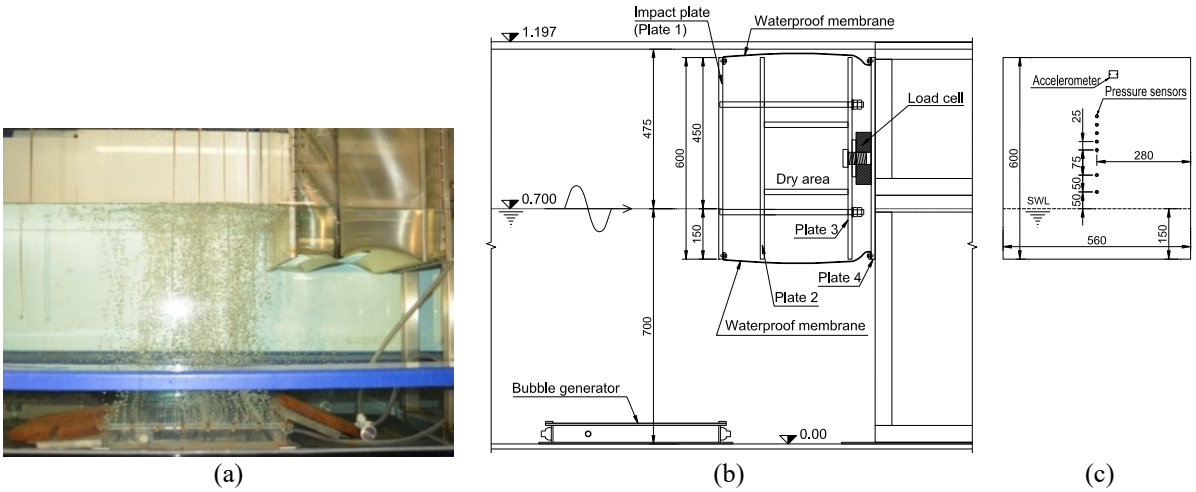

(a) (b) (c)

Figure 1: (a, b) Side view of the tested model in the 35 m long wave flume; (c) Configuration of instrumentation on the impact wall. Unit in mm.

2.1.2 Wave conditions

Focused wave groups were generated using NewWave (Tromans et al., 1991) focusing with an underlying JONSWAP spectrum ($\gamma = 3.3$). A focusing technique was applied to generate different types of wave impact by changing the focus location X_f (Kimmoun et al., 2010). Wave conditions were scaled from prototype by a factor of 1:65 of the 100 year extreme significant wave height at the Cleeton platform in the Southern North Sea (Williams, 2008). Four different types of wave impact were generated by changing the focal location from an absorbing piston paddle in the wave flume. The wave paddle is 0.5 m wide by 1 m high. The distance between the front impact plate (Plate 1) and the wave paddle is 26.9 m. The target focus points are located at $X_f = 28.54$ m, 28.84 m, 29.04 m and 29.44 m from the wave paddle for the broken, high-aeration, flip-through and slightly breaking waves, respectively. The tested wave impacts are:

(a) Broken wave impact: $X_f = 28.54$ m (Figure 2a). This wave breaks near the front face of the wall. This produces a small aerated water mass which hits the wall and is similar to that described by Bullock et al. (2007).

(b) High aeration wave impact: $X_f = 28.84$ m (Figure 2b). At impact, the wall and wave enclose a combined cloud of bubbles and large air pocket (Bullock et al., 2007).

(c) Flip-through wave impact: $X_f = 29.04$ m (Figure 2c). At impact, uprush on the wall causes a jet to rush vertically upwards just before the crest hits the wall (Bredmose et al., 2009; Kimmoun et al, 2010).

(d) Slightly breaking wave: $X_f = 29.44$ m (Figure 2d). This has a higher run-up than its crest, which is slightly broken when it reaches the wall (Bullock et al., 2007).

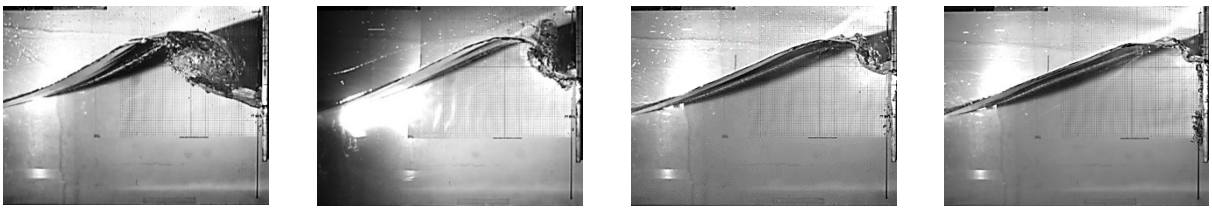

(a) Broken wave (b) High aeration wave (c) Flip-through wave (d) Slightly breaking wave

Figure 2: Four tested wave profiles.

3 Results and discussion

3.1 Characteristics of wave impacts in pure water

3.1.1 Broken wave impact in pure water

Figure 3(a,b,c) presents typical time-histories of acceleration and force under broken wave impact (focus distance $X_f = 28.54$ m) on the wall in pure water. Time $t = 0$ s corresponds to the time of maximum force. In this case, the wave breaks just as it hits the wall. Accelerations up to $3g$ were recorded for the broken wave impacts and are presented in Figure 3a. The maximum impact force due to the broken wave for this particular test was 1.07 kN (Figure 3b). The low frequency oscillation superimposed on the force time history is found to be close to the natural frequency of the model ($f_N = 40$ Hz). This low frequency oscillation was observed in all the force time histories of the broken wave impacts. Due to the chaotic nature of the turbulent flow associated with the broken wave, there is considerable randomness apparent in the pressure time history as can be seen in Figure 3c. At level $z/d = 0.32$, there was a high impact pressure of 0.27 bar (the highest value that was observed for broken waves) at $t = -8.71$ ms (see Figure 3c). Many other test runs of broken wave impacts show high impact pressures up to 0.22 bar that were attained at early times, around $t = -100$ ms. There are high frequency oscillations superimposed on the pressure signals. These oscillations are likely to be due to the alternate expansion and compression of the dense cloud of bubbles seen in the image sequence of Figure A-1 in Appendix A.1, and also noted by Hattori et al. (1994) and Bullock et al.

(2007). Figure A-1 shows sequential snapshots of the broken wave impact, and a small volume of aerated water is evident. The wave approaches from the left-hand side and the wall is located at the right-hand end of each snapshot. As shown in Figure A-1, at t = -100 ms, the breaking wave hit the wall, causing high random impact pressures between t = -100 ms and t = 0. Repeatability of acceleration, force and pressures observed in five broken wave impact tests is presented in Figure B-1 in Appendix B.1. Acceleration and pressures on the wall have significant variation between repeats (Figure B-1a and Figure B-1c-h), but the total force on the wall seems to be repeatable (Figure B-1b).

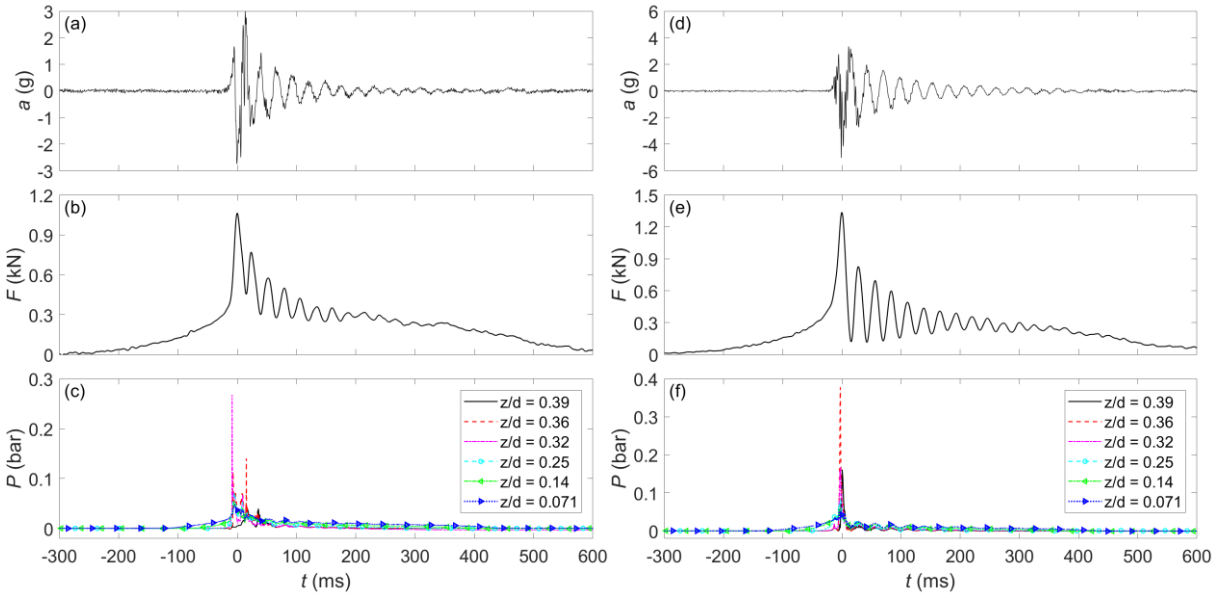

Figure 3: Typical time histories of acceleration, force and pressures in pure water under: (a,b,c) Broken wave impact; (d,e,f) High aeration wave impact.

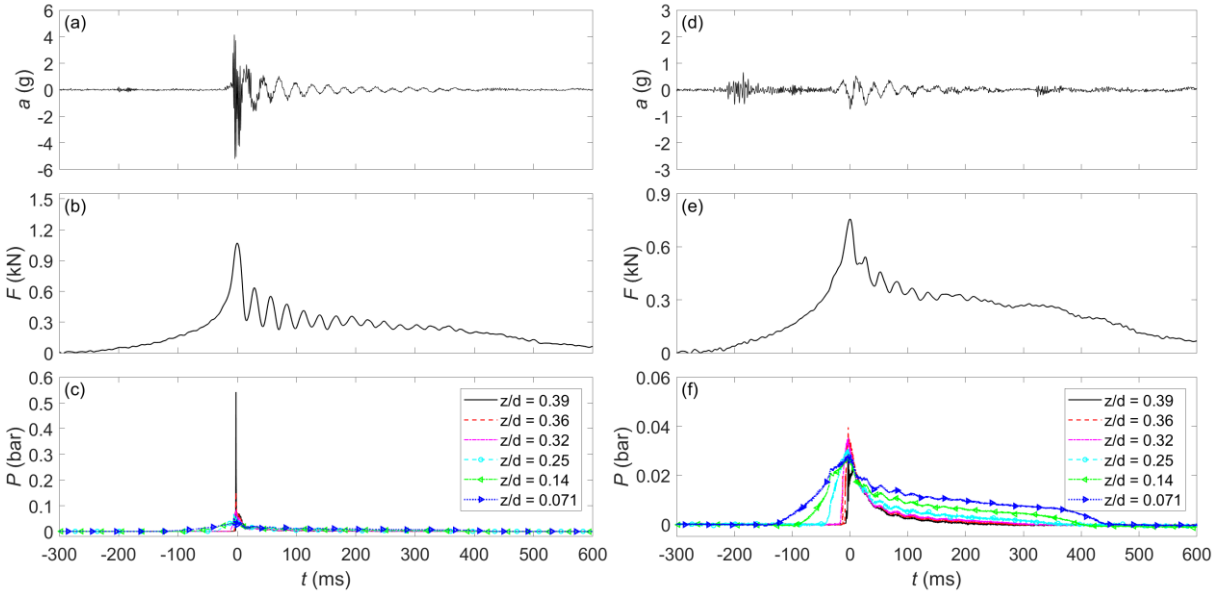

Figure 4: Typical time histories of acceleration, force and pressures in pure water under: (a,b,c) Flip-through wave impact; (d,e,f) Slightly breaking wave impact.

3.1.2 High aeration wave impact in pure water

Under the high aeration wave impact (focus distance X_f = 28.84 m), the maximum acceleration of the wall is up to 3.5g for the case illustrated in Figure 3d. The time-history of the measured force on the wall under high aeration impact is presented in Figure 3e. The low frequency oscillations of the acceleration and force traces after the impact (between t = 0 ms and t = 500 ms in Figure 3d,e) can be seen and they are identical to the 40 Hz natural frequency of the structure. Figure 3f presents

associated time-histories of pressures on the wall at different levels for the test case presented in Figure 3d,e. Higher impact pressures, in comparison with the previous wave impact types, are found and the time of peak pressure for each gauge is now nearly simultaneous under this wave impact type. The low frequency oscillation found in acceleration and force traces can also be observed from the pressure traces under the high aeration wave impact type (seeFigure 3). It is shown that there are high frequency (~170 Hz to 880 Hz) pressure oscillations after the impact (between t = 0 ms and t = 11 ms in Figure 3f). These high frequency oscillations may be due to the acoustic wave reflecting from the flume bottom and/or due to air-pocket and bubble oscillations. Using the theoretical natural frequency of air bubbles in water as derived by Minnaert (1933) and Hattori et al. (1994), the frequency of oscillation observed here corresponds to air-pocket and bubble radius of between 19.2 mm and 3.7 mm. This behaviour of the pressure time histories after the impact is similar to the previous findings for large air-pocket wave impacts (Hattori et al., 1994) or high aeration wave impacts (Bullock et al., 2007), where the variation of pressure peaks are very large. Figure A-2 shows the high aeration wave impact in sequential snapshots taken from t = -100 ms to t = 50 ms. It can be seen that the wave crest started to overturn at t = -100 ms and as time proceeded the jet of the breaking wave hit the wall and entrapped a large air volume and a cloud of bubbles (see at time between t = -30 ms and t = -10 ms). Measurements of acceleration, force and pressures on the wall are shown in Figure B-2 for five high aeration wave impact tests. The total force on the wall shows a high level of repeatability for the high aeration wave impact (Figure B-2b). Low frequency oscillation after impact on the acceleration and pressure traces is found to be repeatable, but the maximum acceleration and the impact pressure show some variation (Figure B-2a&c-h).

3.1.3 Flip-through wave impact in pure water

Flip-through impacts occur when the wave front is kept from striking the wall by a jet coming from below and this type lies between air-pocket impact and sloshing. Flip-through impact was first identified by Cooker and Peregrine (1990) from fully non-linear potential flow computation. Figure 4(a,b,c) presents time histories of the accelerations, force and pressures of a flip-through impact test case which caused the largest impact pressure (0.54 bar at level z/d = 0.39 in Figure 4c) obtained from any experiment presented here. The focus distance of X_f = 29.04 m was used to generate this flip-through wave impact type. The maximum acceleration of the wall on impact was recorded up to 4.5g for this particular case (Figure 4a). Similar to the broken wave and high aeration impacts, evidence of the low frequency oscillation (~37 Hz), due to the natural frequency vibration of the impact wall, was found in the acceleration, force and pressure signals under the flip-through impacts. A high frequency oscillation (~620 Hz) was also observed after impact in pressure signals at all measured levels (Figure 4c). This high frequency oscillation may be due to oscillation of 10.6 mm-diameter air bubble or a bubble cloud which was enclosed during the flip-through impact due to turbulence of the water surface. The high frequency oscillation of pressures after impact might also be caused by a sound wave reflected from the flume bed. Phase differences of the high frequency oscillations in the pressure traces were observed and this may be due to the different distances between the pressure sensors and the impact point, where the air bubble was formed and the sound wave started to transmit. Figure A-3 in Appendix A.1 presents snapshots of the flip-through impact at different time instants and it shows clearly the turbulence associated with the flip-through wave impact. Similar to the high aeration wave impact, the total force on the wall is shown to have a high level of repeatability (Figure B-3b). However, acceleration and pressures are not repeatable, except the low frequency oscillation after the impact which is known to be due to the natural frequency vibration of the wall (Figure B-3a&c-h).

3.1.4 Slightly breaking wave impact in pure water

Increasing the focus distance up to X_f = 29.44 m leads to the run-up on the wall being higher than the crest and the crest is slightly broken when it reaches the wall. Figure 4(d,e,f) present accelerations, force and pressures under the slightly breaking wave impact. A maximum acceleration of 0.7 g was recorded after the impact for this particular slightly breaking wave impact (Figure 4d). There is also

a low frequency oscillation evident in the force signal (see Figure 4e) but the amplitude of this oscillation is much lower than that due to other wave impacts (broken, high aeration and flip-through impacts). As can be seen in the pressure time histories presented in Figure 4f, the pressure peak tends to decrease as the level z/d increases, except at the level $z/d = 0.32$ and 0.36 where the wave crest hits the wall causing high pressures. A preceding single impact was found on the pressure trace at level $z/d = 0.36$ that is due to slight breaking of the wave crest which can be seen in the snapshots in Figure A-4 in Appendix A.1. Acceleration, total force and pressures on the wall due to five slightly breaking wave impacts are illustrated in Figure B-4 in Appendix B.1, and show clear lack of repeatability of acceleration and pressures on the wall as findings from other wave impact types have shown (Figure B-4a&c-h). However, total force on the wall seems to be repeatable for the slightly breaking wave impact, see Figure B-4b.

3.2 Characteristics of wave impacts in aerated water

Figure 5 and Figure 6 illustrate typical time histories of acceleration, force and pressures on the wall in the aerated water for the four wave impact types. Comparisons of water surface elevation time histories between the tests in pure and aerated water have been made and presented in Figure 7 for the four wave impact types at two different flume locations. Figure A-5 to A-8 in Appendix A.2 show the sequential snapshots during the wave impacts in aerated water.

Figure 5 (a,b,d,f) and Figure 6(a,b,d,f) show that during the impacts, the low frequency oscillation (~37 Hz) is evident in the acceleration and force traces but its amplitude is smaller than that in pure water. Looking at the pressure traces in Figure 5(c,f) and Figure 6(c,f), there are no significant high pressure peaks such as obtained in pure water under the impacts presented in Section 3.1. High frequency oscillations after the impacts were also observed in the pressure traces particularly evident in Figure 5f and these oscillations are considered to be due to the expansion and compression and pressure wave transmitted through the water-air mixture.

Repeatability of wave impacts in aerated water is presented in Appendix B.2 for four wave impact types. Similar to wave impact in pure water, the total force on the wall shows good repeatability, and the accelerations and pressures are more variable with no clear repeatable behaviour.

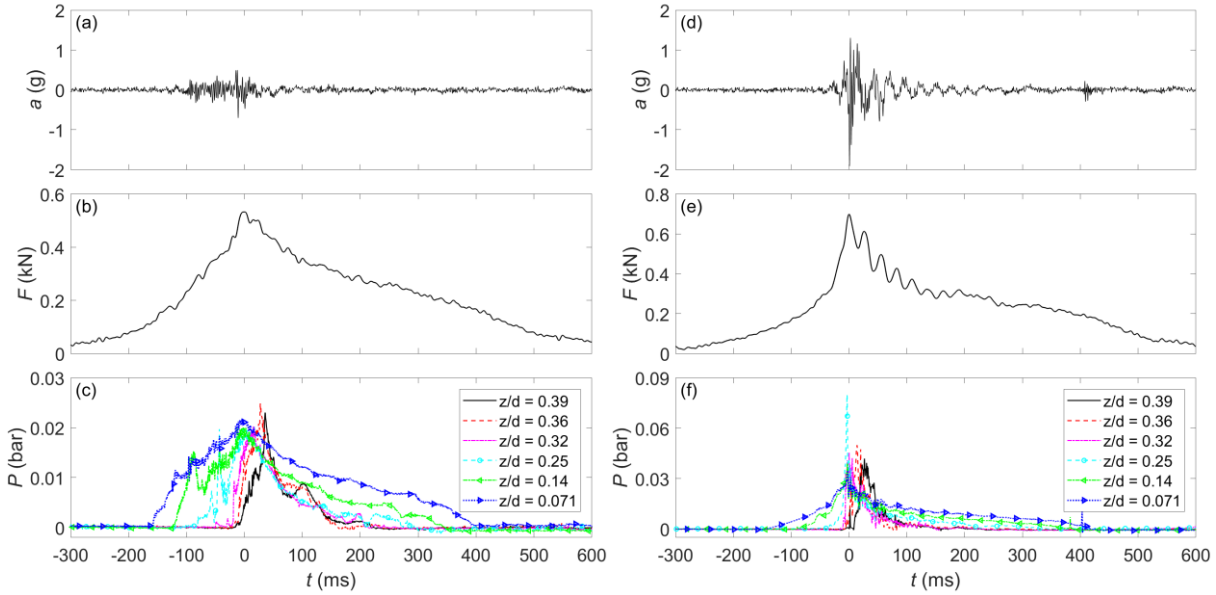

Figure 5: Typical time histories of acceleration, force and pressures in aerated water under: (a,b,c) Broken wave impact; (d,e,f) High aeration wave impact.

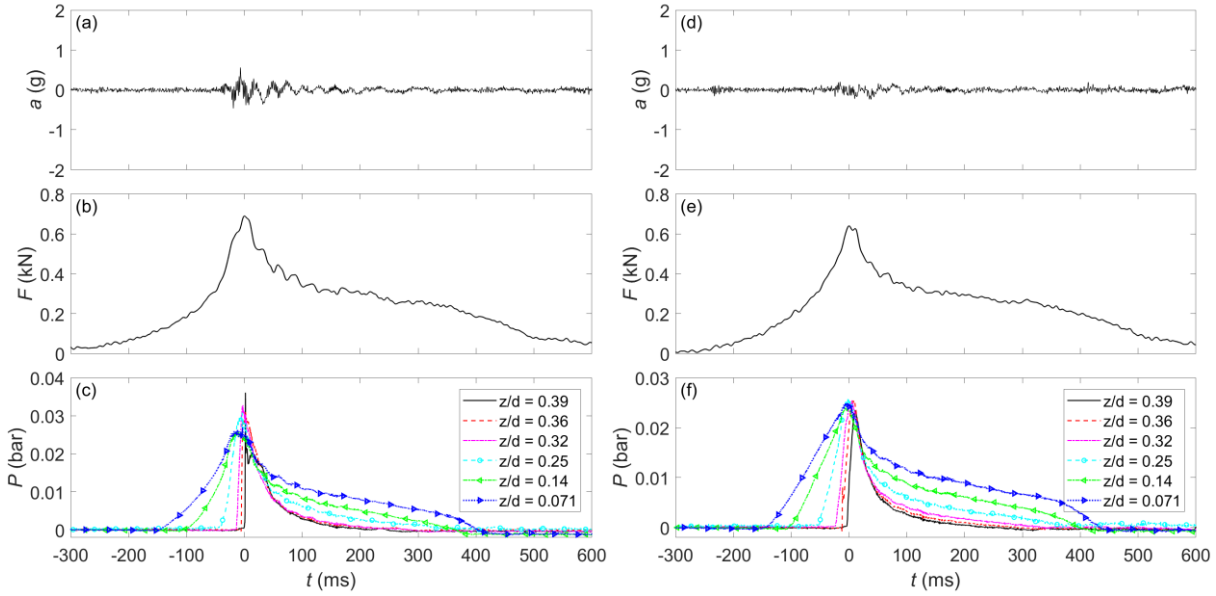

Figure 6: Typical time histories of acceleration, force and pressures in aerated water under: (a,b,c) Flip-through wave impact; (d,e,f) Slightly breaking wave impact.

Water surface elevation time histories of the same wave impact types in pure and aerated water at location x = -0.15 m (x = 0 corresponds to the front of the impact wall) are presented in Figure 7. Air flow expelled from the bubble generator, came into the water body and generated a flow, which was first in the vertical direction and then horizontally. Consequently, there was a surface current opposite to the incoming wave direction. This effect on the incoming waves is clearly shown in Figure 7. It tended to change the incoming wave in the aerated water (dashed line in plots) so that it arrived 0.08 s later than that in the pure water (solid line). Furthermore, it slowed down the wave, leading to an increase in the wave steepness. The difference between the maximum wave crest elevations in pure and aerated waters, at x = -0.15 m, was up to 0.01 m. The disturbance of the wave crest due to the presence of a bubble curtain was studied by Kimmoun et al. (2012) who showed that the disturbance could lead to a small decrease in impact pressure on a vertical wall, such as is found in the experiments presented here.

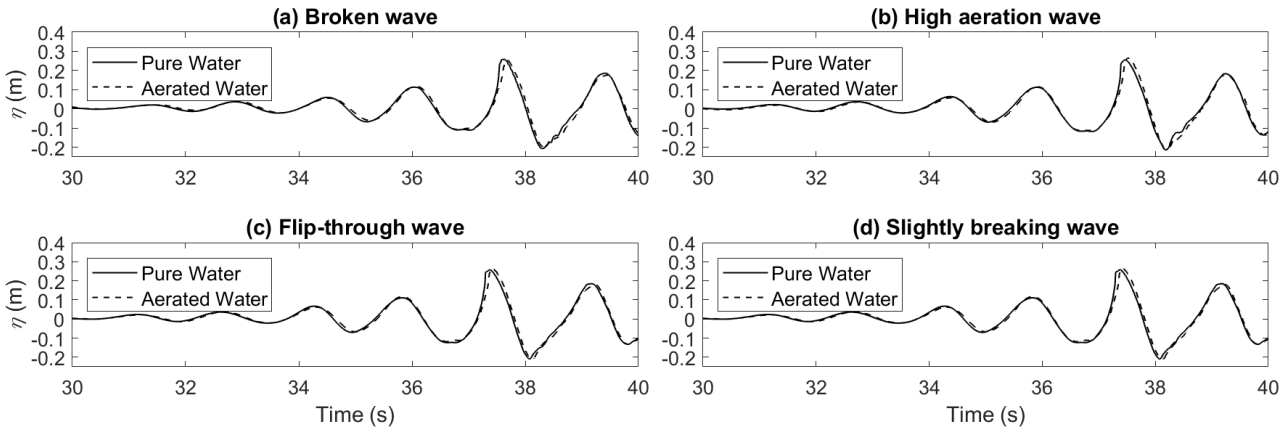

Figure 7: Comparison of time histories of the tested waves in pure and aerated water.

3.3 Wave impact pressure and its impulse

The maximum pressures at various levels on the wall are presented in Figure 8 for all wave impact types in pure and aerated water. The vertical axis is the dimensionless level z/d of the measured points on the wall and the SWL is represented by z/d = 0. The horizontal axis is the logarithm of dimensionless impact pressure, $P_{max}/\rho g d$. The black diamonds are the impact pressures in pure water and the red pluses are the impact pressures in the aerated water with 0.6% of void fraction. The solid and dashed lines join mean values of data points at each level on the wall in pure and aerated water, respectively. Maximum impact pressures were found to occur at elevations above the SWL for

impacts in 0.625 m water depth. It is clearly seen from Figure 8 that there is a significant reduction of the impact pressures from pure water to aerated water. The maximum impact pressures measured in pure water were 0.27 bar, 0.38 bar, 0.56 bar and 0.2 bar for the broken, high aeration, flip-through and slightly breaking wave impacts, whereas those maximum impact pressures were only from 0.03 bar to 0.13 bar for wave impacts in aerated water. The incident wave was also affected by the current and turbulence induced by the bubble generator, which further reduces the impact pressures. Significant reduction of the impact pressure in aerated water was also found in the experimental work of Kimmoun et al. (2012).

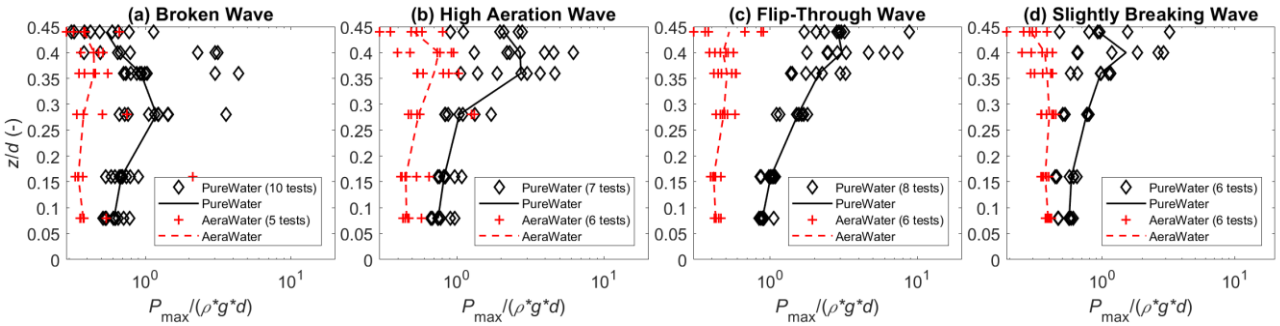

Figure 8: Impact pressures in pure and aerated water.

Figure 9 shows pressure impulses on the vertical wall for pure and aerated water. The impulse value is integrated over the duration of the measured signal (Cooker and Peregrine, 1995). The black diamond markers and solid line are the pressure impulse and its mean values at the measured levels in pure water, respectively. The red plus marker and dashed line are for the aerated water. The results show that the pressure impulses in aerated water are a little smaller than those in pure water for all types of wave impacts (broken, high aeration, flip-through and slightly breaking). Pressure impulses decrease with increasing elevation on the wall for both pure and aerated water. This is because the pressure oscillations were sustained for a long duration.

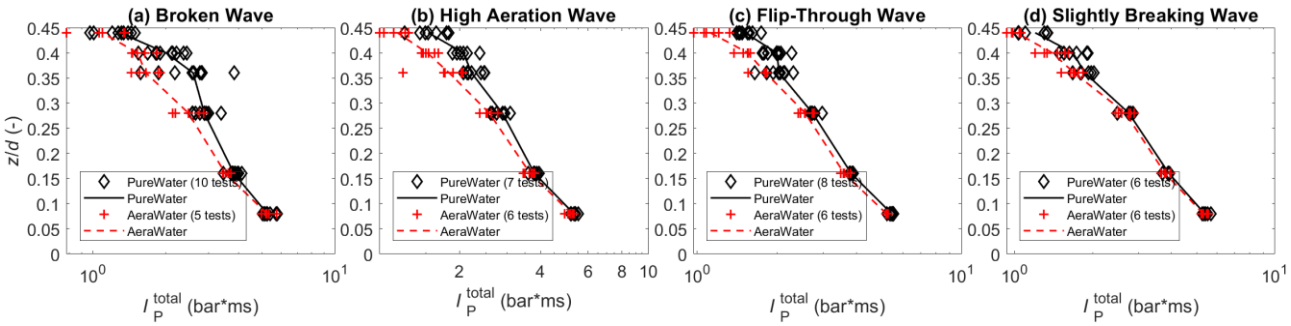

Figure 9: Pressure impulses in pure and aerated water.

3.4 Wave impact force and its impulse

Figure 10 presents the impact forces and force impulses on the wall in pure and aerated water. As seen for the pressure results, impact forces in pure water are significantly higher than in aerated water (Figure 10a). In both pure and aerated waters, the flip-through impact resulted in the highest impact force and the broken wave impact caused the lowest impact force on the hull section. Similar findings were reported by Kimmoun et al. (2012) for a vertical wall and bubble curtain arrangement. In general, the average values of the total force impulses in pure water are higher than those in aerated water but their variation is quite large and in some events the total force impulse in aerated water is larger than that in pure water (Figure 10b).

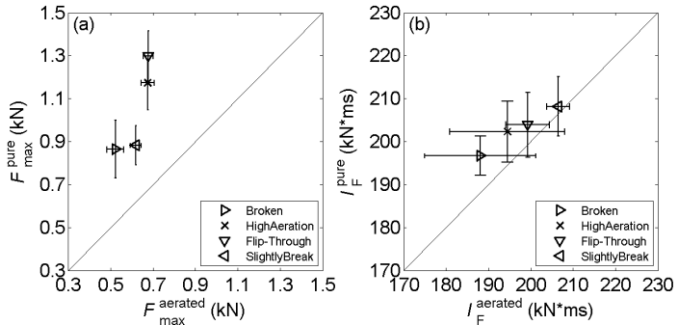

Figure 10: (a) Impact force and (b) force impulse on wall in pure and aerated water.

4 Conclusions

This paper examined the role of aeration in wave impacts. Experimental work was conducted by means of wave impact on a truncated vertical rigid wall (hull section) in pure and aerated water. Wave impacts on a truncated vertical wall, designed to represent a vertical section of an FPSO hull, were explored for various wave impact types, including broken, high aeration (large air pocket), flip-through and slightly breaking wave impacts. It is found that the high aeration and flip-through wave impacts are the most severe impact types and they should be considered for offshore structure design. Post-impact, high frequency oscillations of pressures were observed for wave impacts, and these oscillations are due to repeated compression and expansion of the trapped air between wave front and the truncated wall. Therefore, the fatigue analysis of a section of the hull or whole ship structure may need to assess those local high-frequency loading oscillations.

This study observed that aeration has an important effect on wave impacts. A significant reduction in the hydrodynamic impact loadings (pressure and force) is found for those measured in aerated water compared to those in pure water, though there is almost no reduction of the total loading impulses for wave impacts. Therefore, maximum instantaneous loads calculated for pure water may be conservative in the presence of aerated water in the implication for offshore structure design. Currently, standard design practices (Det Norske Veritas, 2012&2016) have not taken into account aerated water in design. The effects of aeration should be taken into consideration for the offshore environment where wave breaking is commonplace, leading to aerated wave interactions with structures.

Acknowledgements

This study was a part of the FROTH (Fundamentals and Reliability of Offshore sTructure Hydrodynamics) project supported by the Engineering and Physical Science Research Council (EPSRC Grant EP/J012866/1). The FROTH project was led by Plymouth University and the collaborative partners included Oxford University, University of Bath, City University London and the Manchester Metropolitan University. The authors gratefully acknowledge the financial support provided by EPSRC and useful discussions with the project partners.

References

Bredmose, H., A. Hunt-Raby, et al. (2009). "The ideal flip-through impact: experimental and numerical investigation." Journal of Engineering Mathematics **67**(1-2): 115-136.

Bullock, G. N., C. Obhrai, et al. (2007). "Violent breaking wave impacts. Part 1: Results from large-scale regular wave tests on vertical and sloping walls." Coastal Engineering **54**(8): 602-617.

Chan, E. S. and W. K. Melville (1988). "Deep-Water Plunging Wave Pressures on a Vertical Plane Wall." Proceedings of the Royal Society of London A: Mathematical, Physical and Engineering Sciences **417**(1852): 95-131.

Chan, E-S (1994). "Mechanics of deep water plunging-wave impacts on vertical structures." *Coast Eng* **22**:115-133.

Chuang, WL., Chang, KA. & Mercier, R. (2017). "Impact pressure and void fraction due to plunging breaking wave impact on a 2D TLP structure." *Exp Fluids* **58**:68.

Chuang, WL., Chang, KA. & Mercier, R. (2018). "Kinematics and dynamics of green water on a fixed platform in a large wave basin in focusing wave and random wave conditions." *Exp Fluids*, **59**:100.

Cooker, M. J. & Peregrine, D. H. (1990). "Computation of violent wave motion due to waves breaking against a wall." *In Proceedings of the 22nd International Conference on Coastal Engineering*, Delft, The Netherlands, pp. 164–176. ASCE.

Cooker, M. J. and D. H. Peregrine (1995). "Pressure-impulse theory for liquid impact problems." *Journal of Fluid Mechanics* **297**: 193-214.

Guilcher, P.-M., Couty, N., Brosset, L., & Le Touzé, D. (2013). "Simulations of Breaking Wave Impacts on a Rigid Wall at Two Different Scales with a Two-Phase Fluid Compressible SPH Model." *International Society of Offshore and Polar Engineers* **23**(4): 241 - 253

Hattori, M., A. Arami, et al. (1994). "Wave impact pressure on vertical walls under breaking waves of various types." *Coastal Engineering* 22 (1 - 2): 79-114.

Hofland, B., Kaminski, M., & Wolters, G. (2011). "Large scale wave impacts on a vertical wall." *Coastal Engineering Proceedings, 1*(**32**), structures.15. doi:http://dx.doi.org/10.9753/icce.v32.structures.15

Hull, P. and G. Müller (2002). "An investigation of breaker heights, shapes and pressures." *Ocean Engineering* **29**(1): 59-79.

Kimmoun, O., Malenica, et al. (2009). "Fluid structure interactions occurring at a flexible vertical wall impacted by a breaking wave." *Proc. of 19th International Offshore and Polar Engineering Conference,* 21-26 July, Osaka, Japan.

Kimmoun, O., A. Ratouis, and L. Brosset (2012). "Influence of a Bubble Curtain on the Impact of Waves on a Vertical Wall." *Proc. of 22nd International Offshore and Polar Engineering Conference*. International Society of Offshore and Polar Engineers, 17-22 June, Rhodes, Greece.

Lafeber, W., H. Bogaert, et al. (2012). Comparison of wave impact tests at large and full scale: Results from the sloshel project. *Proc. of 22nd International Offshore and Polar Engineering Conference*. International Society of Offshore and Polar Engineers, 17-22 June, Rhodes, Greece.

Mai, T. (2017). "On the role of aeration, elasticity and wave-structure interaction on hydrodynamic impact loading." *PhD thesis at Plymouth University*. http://hdl.handle.net/10026.1/9884

Mai, T., Greaves, D., Raby, A., Mai, C. (2019). "Aeration effects on offshore structure wave impacts: Part 2. Drop plate impact tests." *Ocean Engineering*. (under review)

Minnaert, M. (1933). "On musical air bubbles and the sounds of runningwater." *Philos. Mag.,* **16,** 235–248.

Oumeraci, H., H. W. Partenscky, et al. (1992). "Impact loading and dynamic response of caisson breakwaters." *Coastal Engineering Proceedings* **1** (23), 1475-1488.

Oumeraci, H., P. Klammer, et al. (1993). "Classification of Breaking Wave Loads on Vertical Structures." *Journal of Waterway, Port, Coastal, and Ocean Engineering* **119**(4): 381-397.

Wienke, J. and H. Oumeraci (2005). "Breaking wave impact force on a vertical and inclined slender pile - theoretical and large-scale model investigations." Coastal Engineering **52**(5): 435-462.

Williams, M. O. (2008). "Wave mapping in UK waters: Supporting document." *Health and Safety Executive*, Research Report RR621, pp 38.

APPENDIX A: VISUALISATION OF WAVE IMPACTS

Table A-1: Description of figures presented in Appendix A.

Figures	Description
Figure A-1	Snapshots of broken wave impact in pure water
Figure A-2	Snapshots of high aeration wave impact in pure water
Figure A-3	Snapshots of flip-through wave impact in pure water
Figure A-4	Snapshots of slightly breaking wave impact in pure water
Figure A-5	Snapshots of broken wave impact in aerated water
Figure A-6	Snapshots of high aeration wave impact in aerated water
Figure A-7	Snapshots of flip-through wave impact in aerated water
Figure A-8	Snapshots of slightly breaking wave impact in aerated water

A.1 Visualisation of wave impacts in pure water

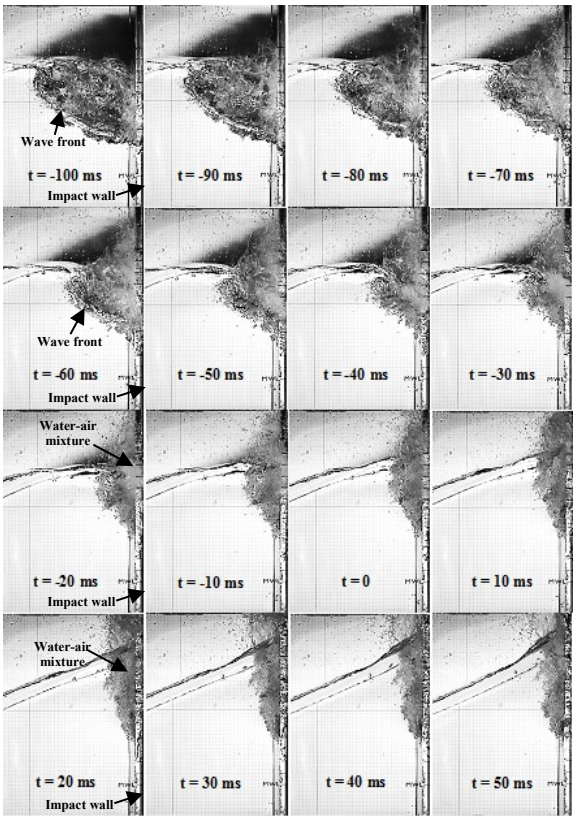

Figure A-1: Snapshots of broken wave impact in pure water. In each snapshot, the wave was coming from the left and the wall was located on the right.

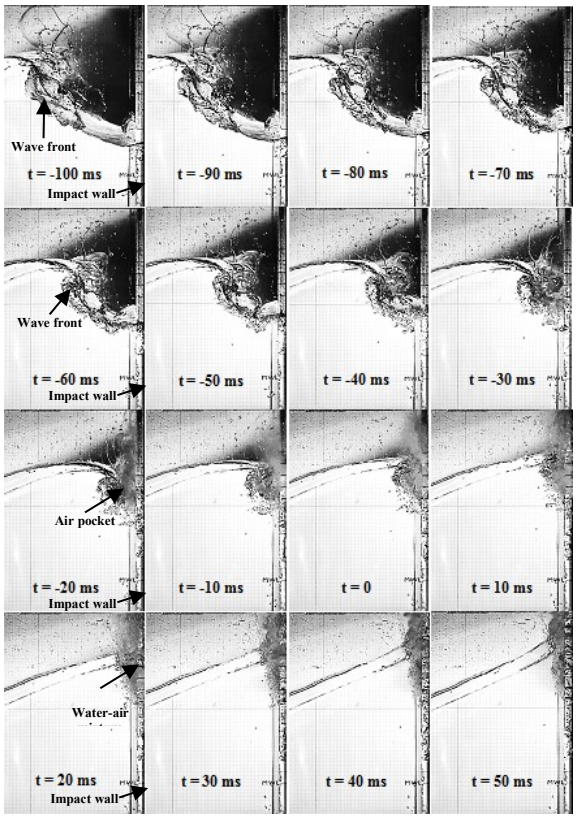

Figure A-2: Snapshots of high aeration wave impact in pure water. In each snapshot, the wave was coming from the left and the wall was located on the right.

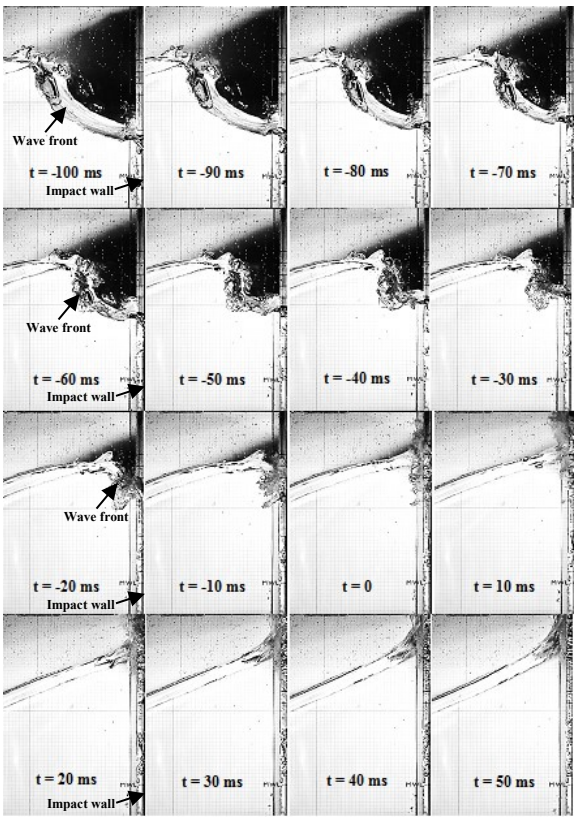

Figure A-3: Snapshots of flip-through wave impact in pure water. In each snapshot, the wave was coming from the left and the wall was located on the right.

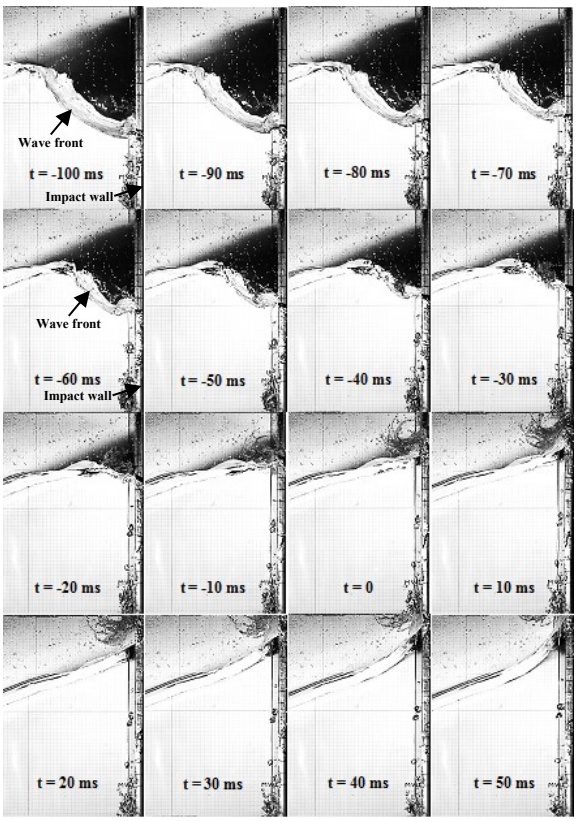

Figure A-4: Snapshots of slightly breaking wave impact in pure water. In each snapshot, the wave was coming from the left and the wall was located on the right.

A.2 Visualisation of wave impacts in aerated water

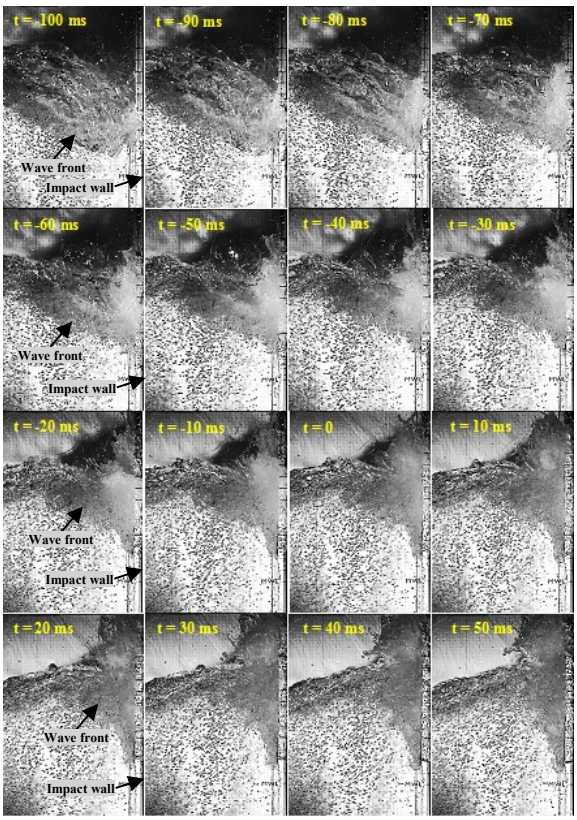

Figure A-5: Snapshots of broken wave impact in aerated water. In each snapshot, the wave was coming from the left and the wall was located on the right.

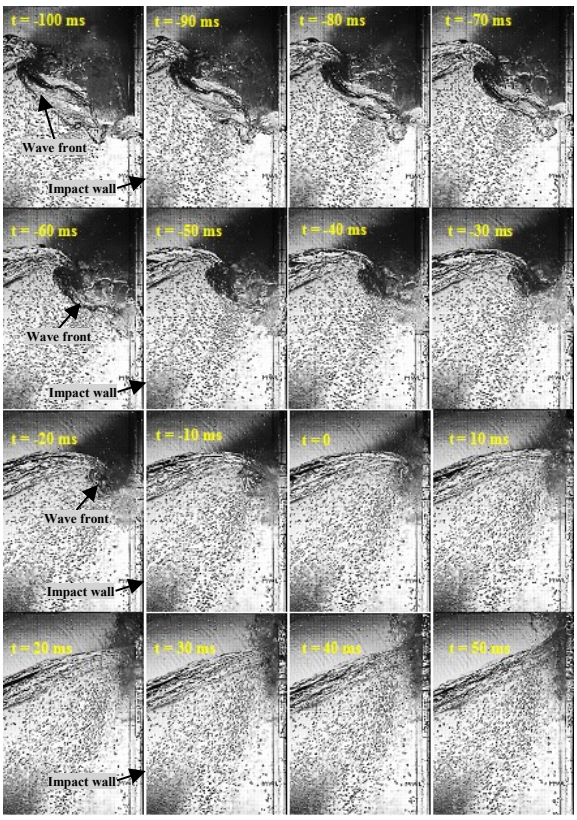

Figure A-6: Snapshots of high aeration wave impact in aerated water. In each snapshot, the wave was coming from the left and the wall was located on the right.

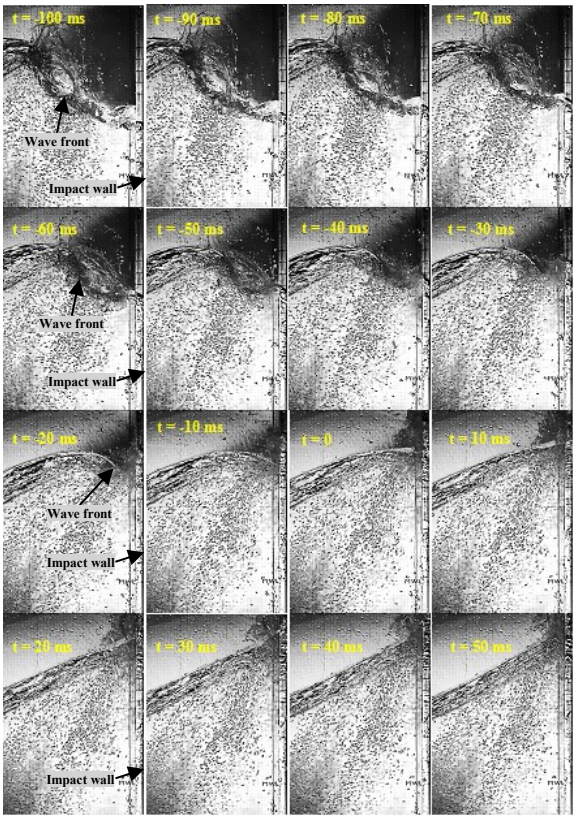

Figure A-7: Snapshots of flip-through wave impact in aerated water. In each snapshot, the wave was coming from the left and the wall was located on the right.

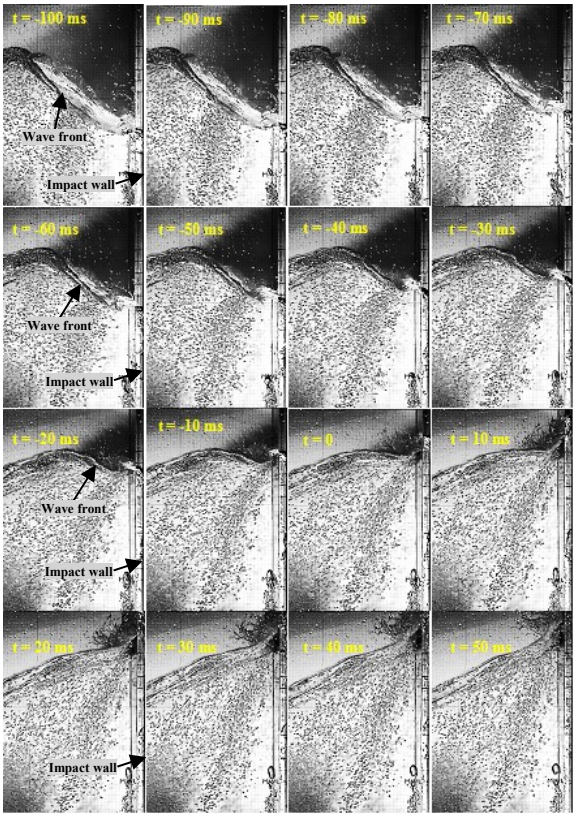

Figure A-8: Snapshots of slightly breaking wave impact in aerated water. In each snapshot, the wave was coming from the left and the wall was located on the right.

APPENDIX B: REPEATABILITY OF WAVE IMPACTS

Table B-1: Description of figures presented in Appendix B.

Figures	Description
Figure B-1	Repeatability of acceleration, force and pressures on the wall under broken wave impact in pure water.
Figure B-2	Repeatability of acceleration, force and pressures on the wall under high aeration wave impact in pure water.
Figure B-3	Repeatability of acceleration, force and pressures on the wall under flip-through wave impact in pure water.
Figure B-4	Repeatability of acceleration, force and pressures the wall under slightly breaking wave impact in pure water.
Figure B-5	Repeatability of acceleration, force and pressures on the wall under broken wave impact in aerated water.
Figure B-6	Repeatability of acceleration, force and pressures on the wall under high aeration wave impact in aerated water.
Figure B-7	Repeatability of acceleration, force and pressures on the wall under flip-through wave impact in aerated water.
Figure B-8	Repeatability of acceleration, force and pressures the wall under slightly breaking wave impact in aerated water.

B.1 Repeatability of wave impacts in pure water

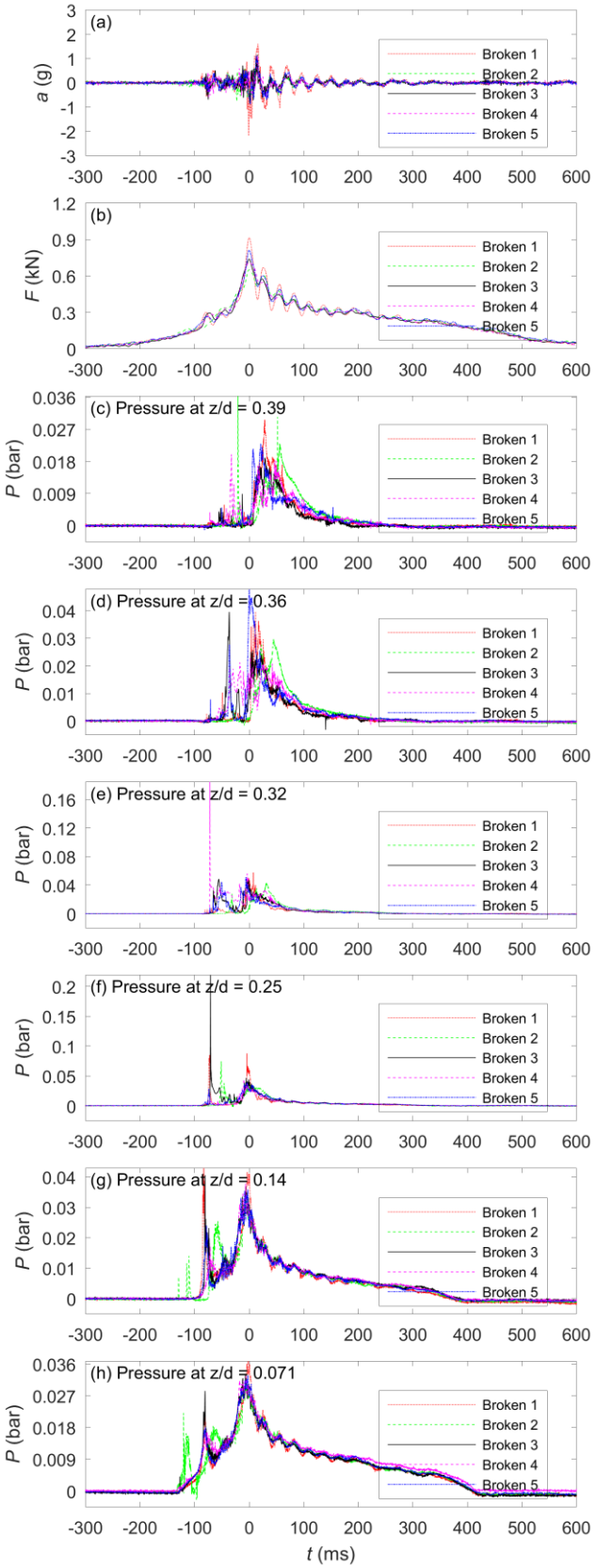

Figure B-1: Repeatability of acceleration, force and pressures on the wall under broken wave impact in pure water.

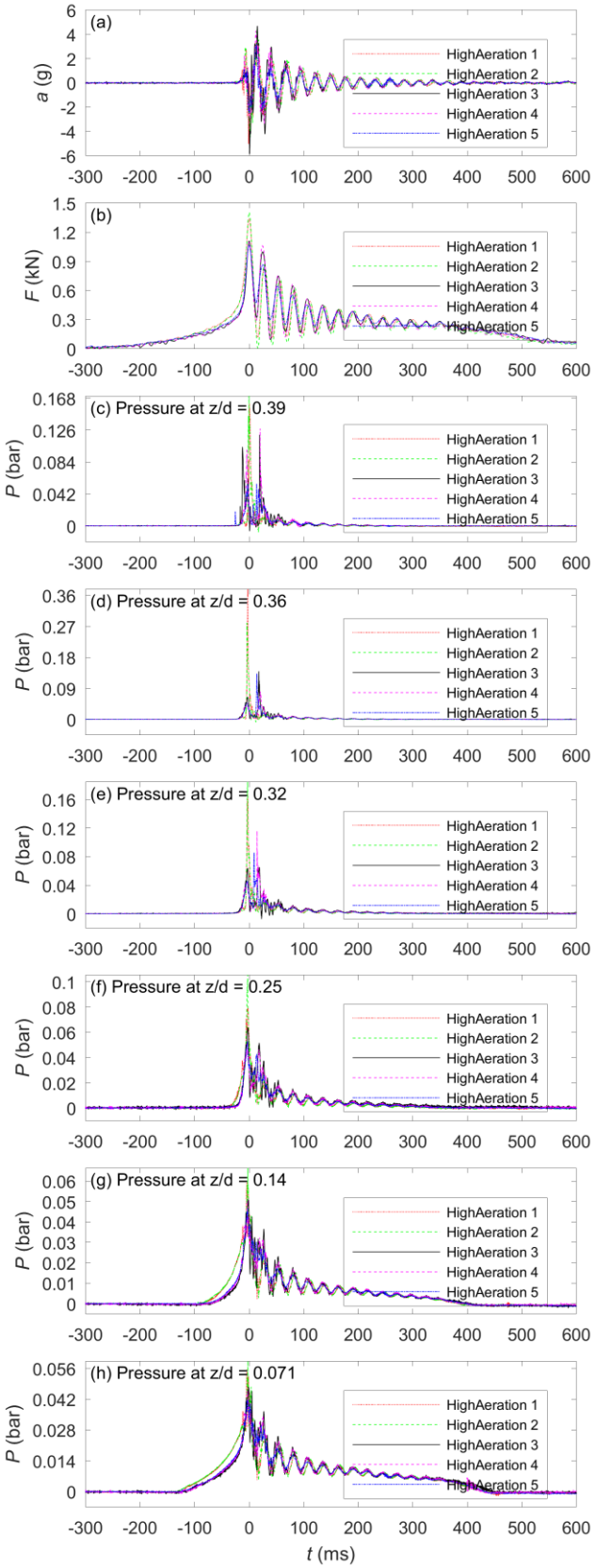

Figure B-2: Repeatability of acceleration, force and pressures on the wall under high aeration wave impact in pure water.

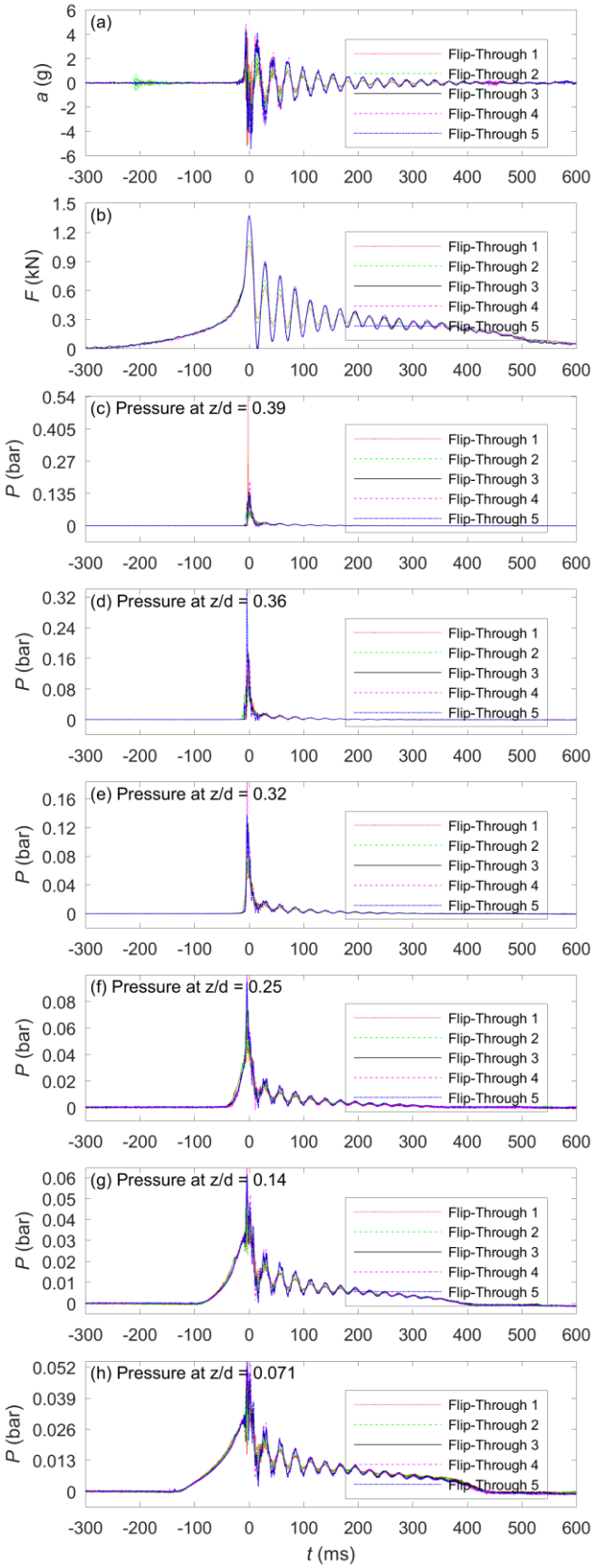

Figure B-3: Repeatability of acceleration, force and pressures on the wall under flip-through wave impact in pure water.

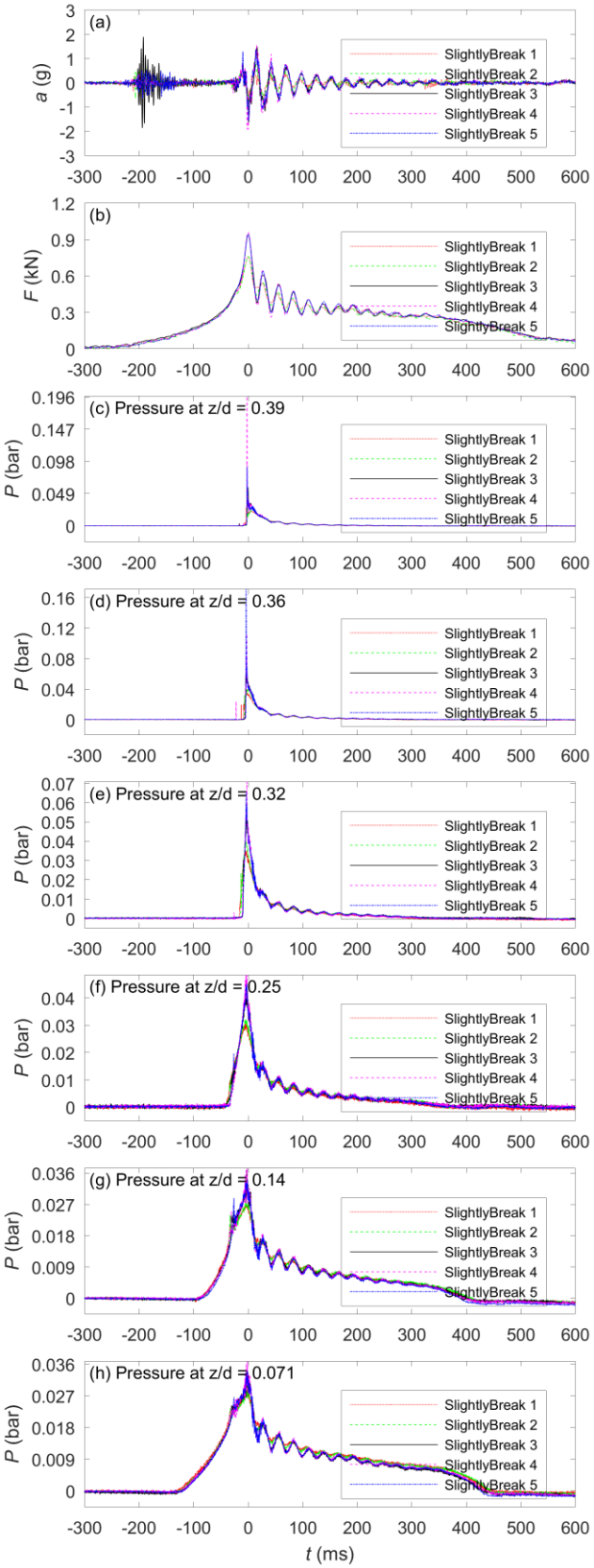

Figure B-4: Repeatability of acceleration, force and pressures the wall under slightly breaking wave impact in pure water.

B.2 Repeatability of wave impacts in aerated water

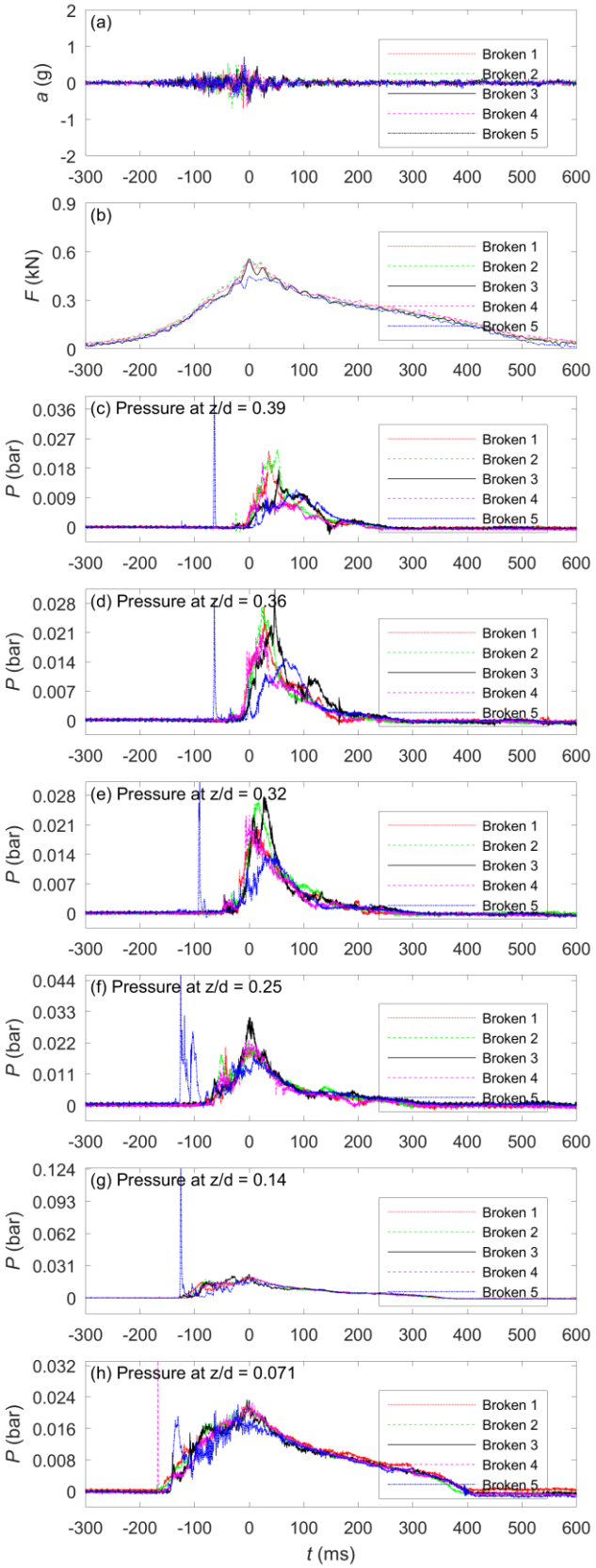

Figure B-5: Repeatability of acceleration, force and pressures on the wall under broken wave impact in aerated water.

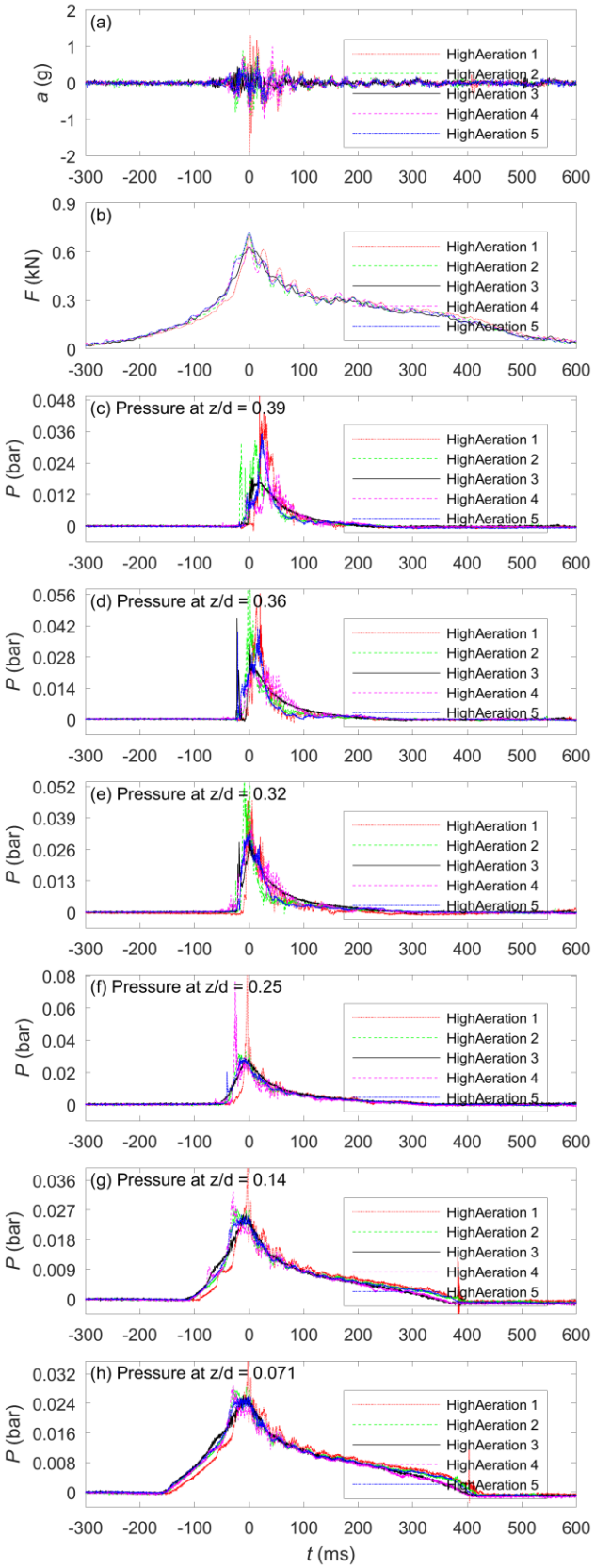

Figure B-6: Repeatability of acceleration, force and pressures on the wall under high aeration wave impact in aerated water.

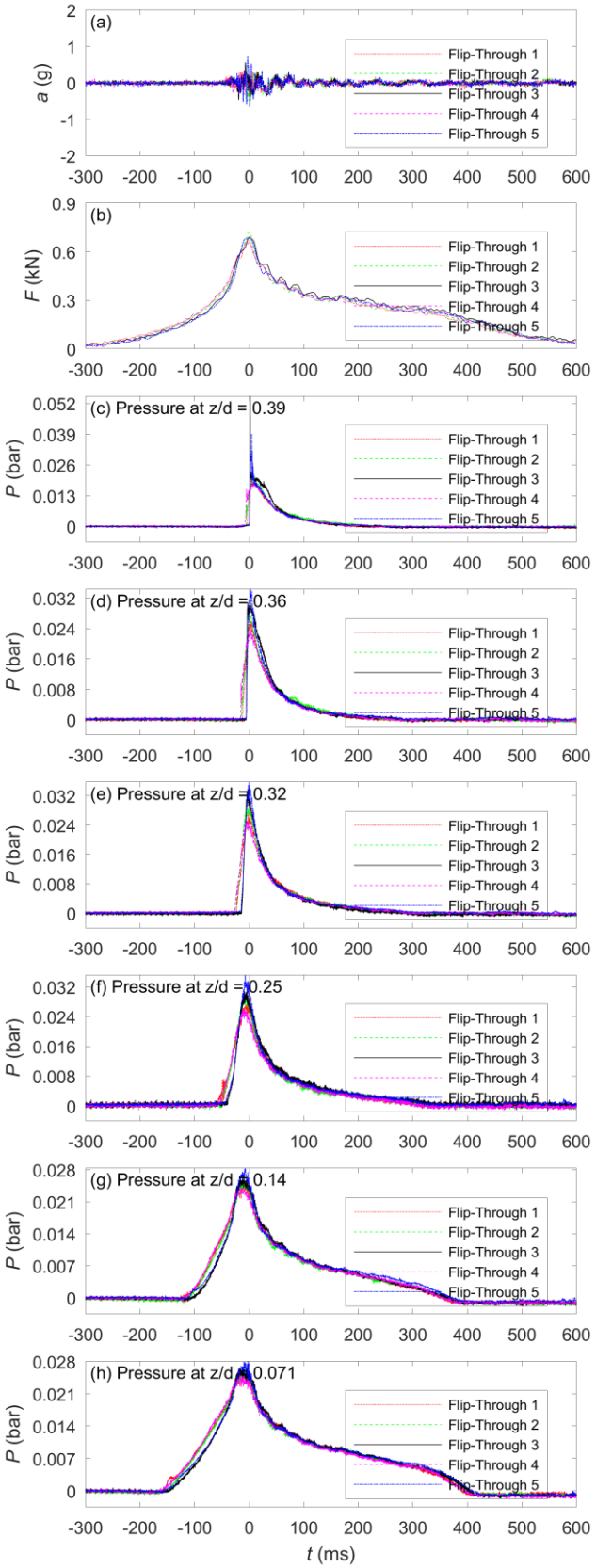

Figure B-7: Repeatability of acceleration, force and pressures on the wall under flip-through wave impact in aerated water.

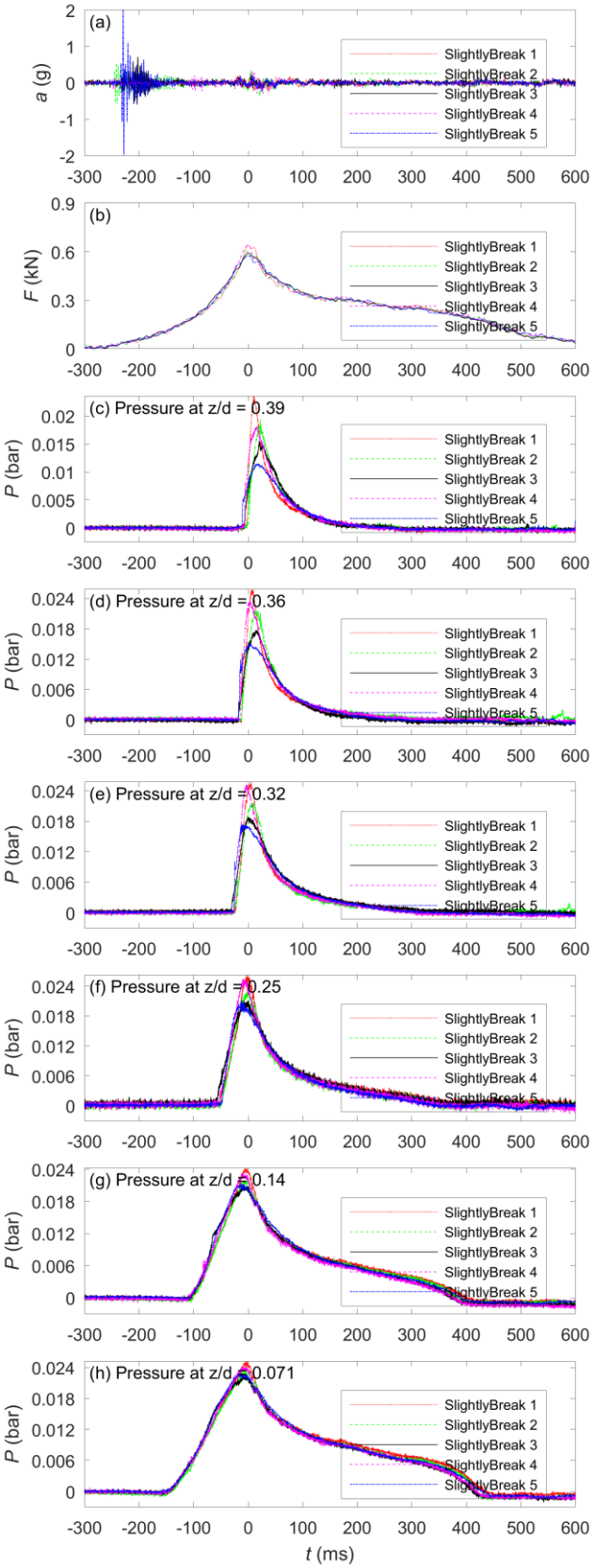

Figure B-8: Repeatability of acceleration, force and pressures on the wall under slightly breaking wave impact in aerated water.